



Discover Generics

Cost-Effective CT & MRI Contrast Agents



WATCH VIDEO

AJNR

High-Resolution Double Inversion Recovery Black-Blood Imaging of Cervical Artery Dissection Using 3T MR Imaging

M.A. Hunter, C. Santosh, E. Teasdale and K.P. Forbes

AJNR Am J Neuroradiol 2012, 33 (11) E133-E137

doi: <https://doi.org/10.3174/ajnr.A2599>

<http://www.ajnr.org/content/33/11/E133>

This information is current as
of June 20, 2025.

TECHNICAL NOTE

M.A. Hunter
C. Santosh
E. Teasdale
K.P. Forbes

High-Resolution Double Inversion Recovery Black-Blood Imaging of Cervical Artery Dissection Using 3T MR Imaging

SUMMARY: We performed high-resolution DIR-BBI of the cervical arteries at 3T in 19 subjects with cervical dissection. It offered excellent visualization of both the lumen and arterial wall, allowing detection of the primary and secondary features of dissection. We suggest that this is a highly useful technique for diagnosis of cervical dissection, either routinely or in equivocal cases of suspected dissection. It also offers further insight into the pathogenesis of this disorder.

ABBREVIATIONS: BBI = black-blood imaging; CA = carotid artery; CTA = CT angiography; DIR = double inversion recovery; MCA = middle cerebral artery; PCA = posterior cerebral artery; PICA = posterior inferior cerebellar artery; VA = vertebral artery

DIR-BBI has proved to be an excellent technique for structural assessment of the vascular system, nulling signal intensity from flowing blood and perivascular fat. When performed with a surface coil at 3T, it offers a high-resolution assessment of the cervical artery wall and lumen. The technique has been widely used for assessment of carotid atherosclerotic plaque, allowing plaque subcomponents and substructural changes to be identified.¹

We were interested in applying this technique to cervical artery dissection, a pathology that arises in the arterial wall, to see if DIR-BBI might either assist in the diagnosis and/or add to the known pathogenesis and imaging appearances of this condition. Dissection is increasingly recognized as an underlying cause of stroke,²⁻⁴ which is of significant importance because it is treatable. Various imaging modalities have been used to diagnosis this condition, including digital subtraction angiography⁵ CTA,⁶ and MR imaging (MR angiography or T1-weighted fat-saturated imaging).⁷ The diagnosis of dissection can be challenging for all modalities, often relying on secondary luminal findings. Only CTA and MR imaging can assess the primary site of pathology, the arterial wall, though MR imaging offers a much higher contrast resolution for detection of hemorrhage.

Methods and Technique

We performed DIR-BBI of the cervical arteries in subjects with arterial dissection. A high-resolution approach was used, with 3T MR imaging (Signa Excite; GE Healthcare, Milwaukee, Wisconsin) and a surface coil (phased-array 4-channel; Herman Flick, Flick Engineering Solution BV, the Netherlands). 2D time-of-flight angiography of

the neck vessels was used to plan axial 2D BBI (T1-weighted and T2*-weighted).

We applied the technique to 19 subjects (12 men, 7 women; mean age, 47 ± 16 years) with cervical artery dissection in at least 1 vessel, confirmed by CTA (64-section Brilliance CT scanner; Philips Healthcare, Best, the Netherlands) (0.625-mm sections; bolus tracking, 75 mL of contrast at 5 mL/s). Each of the 4 cervical arteries on CTA and BBI was independently reviewed for signs of dissection: 1) intimal flap or double lumen, 2) wall thickening \pm T1 hyperintensity of subacute hemorrhage (BBI only), and 3) stenosis, occlusion, or pseudoaneurysm. A conclusion on the presence or absence of dissection was reached for each vessel (CTA, 1 observer; MR imaging, 2 observers, by consensus), and any other potentially relevant observations were noted. Statistical analyses were performed by using the Statistical Package for the Social Sciences software (SPSS, Chicago, Illinois).

Results

Demographics, clinical findings, and brain imaging findings are summarized in Table 1. Vascular findings are summarized in Table 2. MR imaging was performed a median of 4 days after CTA (interquartile range, 1–5 days).

There was no significant difference between CTA and BBI in the number of subjects or individual vessels with dissection (subjects: CTA, $n = 17$; BBI, $n = 19$; vessels: CTA, $n = 20$; BBI, $n = 24$; McNemar test: $P > 0.05$). (On CTA review, 2 subjects were thought to show imaging features that could have resulted from atherosclerosis or dissection).

MR imaging detected more intimal flaps or double lumen (MR imaging, $n = 15$; CTA, $n = 7$; McNemar test, $P < .03$) (Fig 1A, -B). Wall thickening was more commonly identified on MR imaging (MR imaging, $n = 24$; CTA, $n = 18$; McNemar test, $P < .04$), and T1 hyperintensity, in keeping with hematoma, was noted in all dissected vessels (Fig 3), while T2* was decreased in 3 (Fig 4). In 5, hematoma was localized as subintimal (VA, $n = 3$; CA, $n = 2$) (Fig 5), and in 1, it was as intramedial.

There was no difference in the ability of CTA and MR imaging to detect occlusion (CTA, $n = 8$; MR imaging, $n = 7$) or stenosis (CTA, $n = 13$; MR imaging, $n = 15$) (McNemar test, no significant difference). A pseudoaneurysm was seen in only 1 dissected CA, on both modalities (Fig 2A, -B).

Observational note was made of T2 hyperintense periadventitial

Received November 21, 2010; accepted after revision February 4, 2011.

From the Department of Radiology (M.A.H.), Royal Alexandra Hospital, Paisley, United Kingdom; and Department of Neuroradiology (C.S., E.T., K.P.F.), Institute of Neurological Sciences, Glasgow, United Kingdom.

Paper previously presented at: Annual Meeting of the American Society of Neuroradiology, May 31–June 5, 2008; New Orleans, Louisiana.

Please address correspondence to Mark A. Hunter, MD, Department of Radiology, Royal Alexandra Hospital, Corsebar Rd, Paisley, PA2 9PN, United Kingdom; e-mail: markandrew.hunter@gmail.com

<http://dx.doi.org/10.3174/ajnr.A2599>

Table 1: Demographics: clinical and brain imaging findings

Subject	Sex	Age (yr)	Neurology	Antecedents	Brain Imaging Findings
1	M	39	Dizziness and diplopia		Established right PICA infarct, recent right PCA infarct
2	F	28	Vertigo, diplopia, and left sensory disturbance		Right midbrain infarct
3	M	51	Right sensory disturbance with left Horner syndrome	Working on overhead light	Lateral medullary infarct
4	M	75	Left facial weakness with expressive dysphasia	Prior transient ischemic attack, smoker	Left occipital infarct
5	M	65	Ataxia, dysphonia, left sensory disturbance	Hypertensive, type 2 diabetes, ex-smoker	Left medullary infarct
6	F	35	Top of basilar syndrome		Right cerebellar and bilateral thalamic infarct
7	M	44	Dysarthria, left homonymous hemianopia		Left occipital infarct
8	M	41	Right hemiparesis dysarthria and eye movement disorder		Left PCA infarct
9	M	32	Dysarthria, ataxia, and photophobia	Playing soccer at time	Right occipital infarct
10	F	71	Diplopia and dizziness	Hypertensive	Bilateral cerebellar and pontine infarcts
11	M	40	Vertigo, right weakness, dysarthria, and nystagmus		Right cerebellar infarct
12	F	26	Left facial droop and ptosis	Ehlers Danlos syndrome type 1	Left thalamic and bilateral cerebellar infarcts
13	F	19	Collapse, left weakness; dysarthria and homonymous hemianopia	Weak history of trauma, on injectable contraceptive	Right MCA territory infarct
14	M	60	Left sensorimotor, left homonymous hemianopia		Right total anterior circulatory stroke
15	F	64	Right weakness and dizziness		Right MCA territory infarct
16	M	45	Left Horner syndrome	Heavy laborer with prior chiropractic treatment	
17	M	68	Right weakness		Left parietal and insular infarct
18	F	55	Right weakness and dysphasia		Left basal ganglia infarct
19	M	48	Right weakness and dysphasia		Left MCA territory infarct

edematous signal-intensity change, which tracked into the adjacent parenchyma (dissected vessels, $n = 20$; normal vessels, $n = 0$; χ^2 test, $P < .001$) (Fig 6).

Discussion

This study confirms that BBI is a useful technique for detection of the pathologic findings of dissection, allowing a confident diagnosis to be made.

We chose to perform this technique on subjects with known dissection, as confirmed by CTA, providing a high concentration of pathologic vessels on which to evaluate this sequence. While our study was not designed to compare the sensitivity and specificity of CTA and MR imaging in diagnosing dissection,⁸ BBI did offer improved detection of intimal flaps and wall thickening, suggesting it might offer some improved sensitivity. This technique allows clear visualization of the vessel lumen: Flowing blood is saturated by inversion pulses, giving a true black-blood appearance, improved over spin-echo sequences and offering a high sensitivity to the detection of intraluminal pathology. It also offers excellent spatial and contrast resolution of the vessel wall, allowing better detection of wall thickening and hemorrhage. High T1 contrast resolution allows detection of subacute hemorrhage. We did notice some variation in the strength of T1 hyperintensity, as yet unexplained and not in our data, related to symptom duration. We included a T2*-weighted sequence

to identify the low signal intensity of deoxyhemoglobin in acute dissection, though the numbers were too small to analyze.

The high-resolution DIR-BBI technique may allow us to examine the pathogenesis of dissection further. The traditional belief is that a tear occurs within the intima, allowing entry of arterial blood, creating a false plane of cleavage. This explains why patients with inherent structural collagen weakness^{9,10} are more prone to the condition, but in total, this accounts for only 1%–5% of those affected; in our series only 1 patient (5%) had such connective tissue disease. Contrary to this theory is that of spontaneous rupture of the vasa vasorum. Following this initial event, dissection can extend either between the intima and media, resulting in stenosis or occlusion, or alternatively and less frequently between media and thinner adventitia, which may lead to pseudoaneurysm formation and occasionally rupture and subarachnoid hemorrhage if intracranial.¹¹ Spontaneous rupture of the vasa vasorum, as an underlying cause of dissection might explain why a flap is uncommonly seen at autopsy. However, we identified a flap in nearly one-third of subjects, suggesting that its presence is more common than previously thought and adding support for an intimal tear as a significant primary pathogenic process of arterial dissection.

With the high-resolution DIR-BBI technique, we found it possible to clearly differentiate intramural hematoma from

Table 2: Vascular imaging findings

Subject	Dissected Vessel	Modality	Lumen ^a	Wall ^b	Vessel Contour	Other
1	RtVA	CTA	Intimal flap	Thickened	Stenosis	
	RtVA	BBI	Intimal flap	Thickened T1 hyperintensity +	Occlusion	Periadvential T2 hyperintensity
2	LtVA	CTA	—	Thickened	Stenosis	
	LtVA	BBI	—	Thickened T1 hyperintensity ++ T2* hypointensity +	Stenosis	
	RtVA	CTA	—	Thickened	Stenosis	
	RtVA	BBI	Intimal flap	Thickened T1 hyperintensity ++	Stenosis	Periadvential T2 hyperintensity
3	LtVA	CTA	—	Thickened	Stenosis	
	LtVA	BBI	—	Thickened T1 hyperintensity ++	Stenosis	Periadvential T2 hyperintensity
4	LtVA	CTA	—	Normal	Stenosis	(Abnormal but equivocal cause)
	LtVA	BBI	—	Thickened T1 hyperintensity ++	Occlusion	Periadvential T2 hyperintensity
5	LtVA	CTA	—	Thickened	Occlusion	
	LtVA	BBI	—	Thickened T1 hyperintensity +	Occlusion	Periadvential T2 hyperintensity
6	LtVA	CTA	—	Thickened	Stenosis	
	LtVA	BBI	—	Thickened T1 hyperintensity ++	Stenosis	
	RtVA	CTA	—	Thickened	Stenosis	
	RtVA	BBI	—	Thickened T1 hyperintensity ++ T2* hypointensity +	Stenosis	
7	RtVA	CTA	—	Thickened	Occlusion	
	RtVA	BBI	—	Thickened T1 hyperintensity +	Occlusion	Periadvential T2 hyperintensity
8	LtVA	CTA	—	Thickened	Stenosis	
	LtVA	BBI	Intimal flap	Thickened T1 hyperintensity ++	Stenosis	Periadvential T2 hyperintensity
9	LtVA	CTA	Intimal flap	Thickened	Occlusion	
	LtVA	BBI	Intimal flap	Thickened T1 hyperintensity + T2* hypointensity +	Stenosis	Periadvential T2 hyperintensity
10	LtVA	CTA	—	Thickened	Occlusion	
	LtVA	BBI	Intimal flap	Thickened T1 hyperintensity +/+ ++	Stenosis	Periadvential T2 hyperintensity
	RtVA	CTA	—	Thickened	Stenosis	
	RtVA	BBI	—	Thickened T1 hyperintensity +	Stenosis	Periadvential T2 hyperintensity
11	RtVA	CTA	Intimal flap	Thickened	Stenosis	(Abnormal but equivocal cause)
	RtVA	BBI	Intimal flap	Thickened T1 hyperintensity +/+ ++	Stenosis	Periadvential T2 hyperintensity
12	LtVA	CTA	—	Thickened	Occlusion	
	LtVA	BBI	Intimal flap	Thickened T2* hypointensity +	Stenosis	Periadvential T2 hyperintensity
13	RtCA	CTA	—	Thickened	Occlusion	
	RtCA	BBI	Intimal flap	Thickened T1 hyperintensity +	Occlusion	Periadvential T2 hyperintensity
14	RtCA	CTA	—	Thickened	Occlusion	
	RtCA	BBI	Intimal flap	Thickened T1 hyperintensity ++	Occlusion	Periadvential T2 hyperintensity
15	LtCA	BBI	Intimal flap	Thickened T1 hyperintensity +	—	Periadvential T2 hyperintensity
	RtCA	CTA	Intimal flap	Thickened	Stenosis	
	RtCA	BBI	Intimal flap	Thickened T1 hyperintensity +	Stenosis	Periadvential T2 hyperintensity
	RtCA	CTA	Intimal flap	Thickened	Stenosis	Pseudoaneurysm
16	RtCA	BBI	—	Thickened T1 hyperintensity ++	Stenosis	Pseudoaneurysm Periadvential T2 hyperintensity
	LtCA	CTA	—	Thickened	Occlusion	
17	LtCA	BBI	Intimal flap	Thickened T1 hyperintensity ++	Stenosis	Periadvential T2 hyperintensity
	LtCA	CTA	Intimal flap	Thickened	Occlusion	
18	LtCA	CTA	Intimal flap	Thickened	Occlusion	
	LtCA	BBI	Intimal flap	Thickened T1 hyperintensity ++	Stenosis	Periadvential T2 hyperintensity
	RtCA	BBI	Intimal flap	Thickened T1 hyperintensity ++	Stenosis	Periadvential T2 hyperintensity
	LtCA	CTA	Intimal flap	Thickened	Stenosis	
19	LtCA	BBI	Intimal flap	Thickened	Stenosis	Periadvential T2 hyperintensity
	LtCA	CTA	Intimal flap	Thickened T1 hyperintensity ++	Stenosis	

^a Intraluminal flap present or absent.

^b Wall characteristics: + indicates moderate; + +, strong.

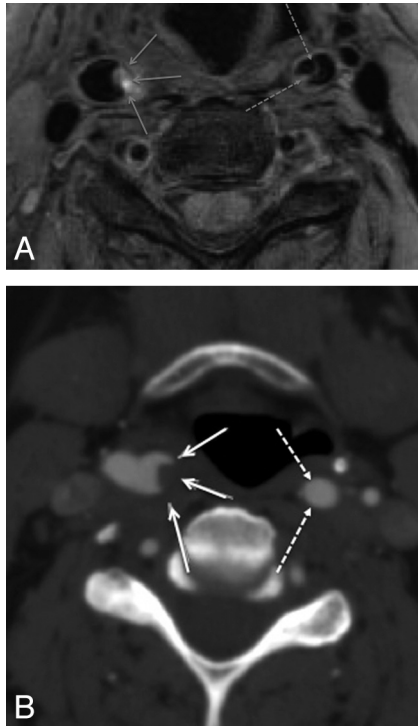


Fig 1. BBL (A) performed 1 day subsequent to CTA (B) demonstrates thrombus within the lumen of the right internal carotid artery (continuous arrows) but also a dissection flap in the left internal carotid artery not appreciated on CTA.

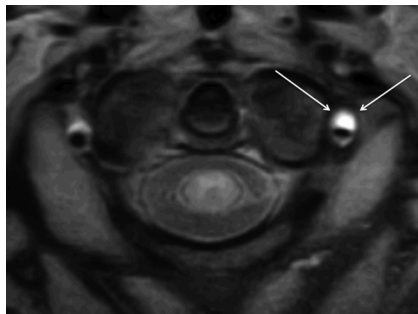


Fig 2. Double inversion recovery BBL demonstrates crescentic intramural high T1 methemoglobin signal intensity (arrows) in the dissected left VA.

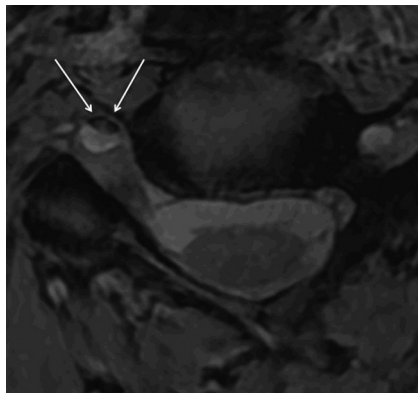


Fig 3. T2* sequence demonstrates crescentic intramural deoxyhemoglobin signal intensity (arrows) in the dissected right VA.

intraluminal thrombus; furthermore, we could sometimes differentiate intramedial from subintimal hemorrhage.

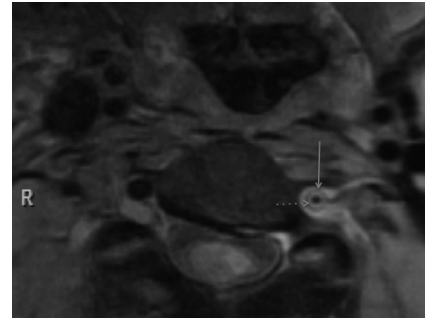


Fig 4. "Target sign" appearance on BBL caused by hematoma in subintimal dissection. The media (continuous arrow) returns low signal intensity; the hematoma (discontinuous arrow), high signal intensity.



Fig 5. Both BBL (A) and CTA (B) demonstrate pseudoaneurysm formation in the skull base of the dissected left internal carotid artery.

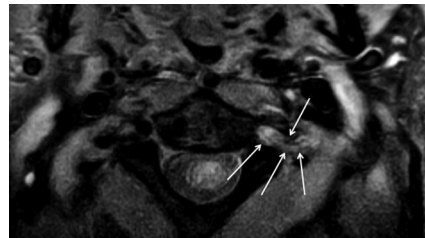


Fig 6. Periaortic signal-intensity change (arrows), presumed due to inflammatory response, surrounding the dissected left VA.

An observational finding commonly noted was T2 hyperintense periaortic signal-intensity change. We postulate that during acute dissection, the artery is surrounded by a variable degree of inflammatory edema. A similar response has been demonstrated in spontaneous coronary artery dissection,^{12,13} and our study confirms similar observation in cervical dissection, as recently reported.¹⁴

Conclusions

3T DIR-BBI is useful in the evaluation of acute cervical artery dissection, offering excellent visualization of the lumen, wall, and periadventitia. This technique could be used either for primary diagnosis or as an adjunct in difficult or inconclusive cases. Furthermore, its high spatial and contrast resolution offers a mode of further exploration into the pathogenesis of dissection.

References

1. DeMarco JK, Ota H, Underhill HR, et al. MR carotid plaque imaging and contrast-enhanced MR angiography identifies lesions associated with recent ipsilateral thromboembolic symptoms: an in vivo study at 3T. *AJNR Am J Neuroradiol* 31:1395–402
2. Schievink WI. Spontaneous dissection of the carotid and vertebral arteries. *N Engl J Med* 2001;344:898–906
3. Schievink WI, Mokri B, O'Fallon WM. Recurrent spontaneous cervical artery dissection. *N Engl J Med* 1994;330:393–97
4. Schievink WI, Mokri B, Whisnant JP. Internal carotid artery dissection in a community: Rochester, Minnesota, 1987–1992. *Stroke* 1993;24:1678–80
5. Provenzale JM. Dissection of the internal carotid and vertebral arteries: imaging features. *AJR Am J Roentgenol* 1995;165:1099–1104
6. Chen CJ, Tseng YC, Lee TH, et al. Multisection CT angiography compared with catheter angiography in diagnosing vertebral artery dissection. *AJNR Am J Neuroradiol* 2004;25:769–74
7. Ozdoba C, Sturzenegger M, Schroth G. Internal carotid artery dissection: MR imaging features and clinical-radiologic correlation. *Radiology* 1996;199:191–98
8. Provenzale JM, Sarikaya B. Comparison of test performance characteristics of MRI, MR angiography, and CT angiography in the diagnosis of carotid and vertebral dissection: a review of the medical literature. *AJR Am J Roentgenol* 2009;193:1167–74
9. Schievink WI, Michels VV, Piepgras DG. Neurovascular manifestations of heritable connective tissue disorders: a review. *Stroke* 1994;25:889–903
10. Brandt T, Orberk E, Weber R, et al. Pathogenesis of cervical artery dissections: association with connective tissue abnormalities. *Neurology* 2001 57:24–30
11. Dziewas R, Konrad C, Dräger B, et al. Cervical artery dissection: clinical features, risk factors, therapy and outcome in 126 patients. *J Neurol* 2003;250:1179–84
12. Bateman AC, Gallagher PJ, Vincenti AC. Sudden death from coronary artery dissection. *J Clin Pathol* 1995;48:781–84
13. Robinowitz M, Virmani R, McAllister HA. Spontaneous coronary artery dissection and eosinophilic inflammation: a cause and effect relationship? *Am J Med* 1982;72:923–28
14. Bachmann R, Nassenstein I, et al. Spontaneous acute dissection of the internal carotid artery: high-resolution magnetic resonance imaging at 3.0 Tesla with a dedicated surface coil. *Invest Radiol* 2006;41:105–11